The Arctic–Atlantic Thermohaline Circulation*

TOR ELDEVIK

Geophysical Institute, University of Bergen, and Bjerknes Centre for Climate Research, Bergen, Norway

JAN EVEN Ø. NILSEN

Nansen Environmental and Remote Sensing Center, and Bjerknes Centre for Climate Research, Bergen, Norway

(Manuscript received 28 May 2013, in final form 15 August 2013)

ABSTRACT

The Atlantic Ocean's thermohaline circulation is an important modulator of global climate. Its northern branch extends through the Nordic Seas to the cold Arctic, a region that appears to be particularly influenced by climate change. A thermohaline circulation is fundamentally concerned with two degrees of freedom. This is in particular the case for the inflow of warm and saline Atlantic Water through the Nordic Seas toward the Arctic that is balanced by two branches of outflow. The authors present an analytical model, rooted in observations, that constrains the strength and structure of this Arctic–Atlantic thermohaline circulation. It is found, maybe surprisingly, that the strength of Atlantic inflow is relatively insensitive to anomalous freshwater input; it mainly reflects changes in northern heat loss. Freshwater anomalies are predominantly balanced by the inflow's partition into estuarine and overturning circulation with southward polar outflow in the surface and dense overflow at depth, respectively. More quantitatively, the approach presented herein provides a relatively simple framework for making closed and consistent inference on the thermohaline circulation's response to observed or estimated past and future change in the northern seas.

1. Introduction

The Atlantic Ocean's thermohaline circulation (THC) carries heat and salt from the tropics to the high northern latitudes (e.g., Wunsch 2002; Kuhlbrodt et al. 2007). It is completed north of the Greenland–Scotland Ridge (GSR) that separates the Nordic Seas and Arctic Ocean—the Arctic Mediterranean—from the North Atlantic (Fig. 1). The warm and saline inflow of Atlantic Water (AW) is totally transformed by atmospheric heat loss and freshwater input as it travels the Arctic Mediterranean (Mauritzen 1996; Rudels et al. 1999). Heat is mainly removed in the Nordic Seas, leading to dense water formation and overturning circulation, while freshwater input maintains an Arctic surface layer that forms an estuarine circulation with the Atlantic-derived water below (Isachsen et al. 2007; Rudels 2010). The cold return flow across GSR is consequently fresh polar water (PW) at the surface and dense overflow water (OW) at depth (Hansen and Østerhus 2000). Whereas the inflow moderates regional climate (Rhines et al. 2008), the polar outflow is a main freshwater source for the Atlantic Ocean (Dickson et al. 2007) and the dense overflow is a main source of North Atlantic deep water (Quadfasel and Käse 2007). The strength, structure, and sensitivity of the THC to anomalous northern heat and freshwater are therefore matters of much interest (Curry and Mauritzen 2005; Serreze et al. 2007; Spielhagen et al. 2011). Constraining the Arctic–Atlantic THC is the purpose of this study.

The combined circulation of heat and salt is generically concerned with two degrees of freedom, as is the described Arctic–Atlantic exchange with one inflow and two outflows across GSR. It can be argued that the present understanding of THC in general and its northern limb in particular does not reflect this fact. Atlantic THC is commonly assessed as one overturning circulation loop (Rahmstorf 1996; Lynch-Stieglitz et al. 2007) and descriptions of water mass transformation

* Bjerknes Centre for Climate Research Publication Number A431.

Corresponding author address: Tor Eldevik, Geophysical Institute, University of Bergen, P.O. Box 7803, 5007 Bergen, Norway. E-mail: tor.eldevik@gfi.uib.no

DOI: 10.1175/JCLI-D-13-00305.1

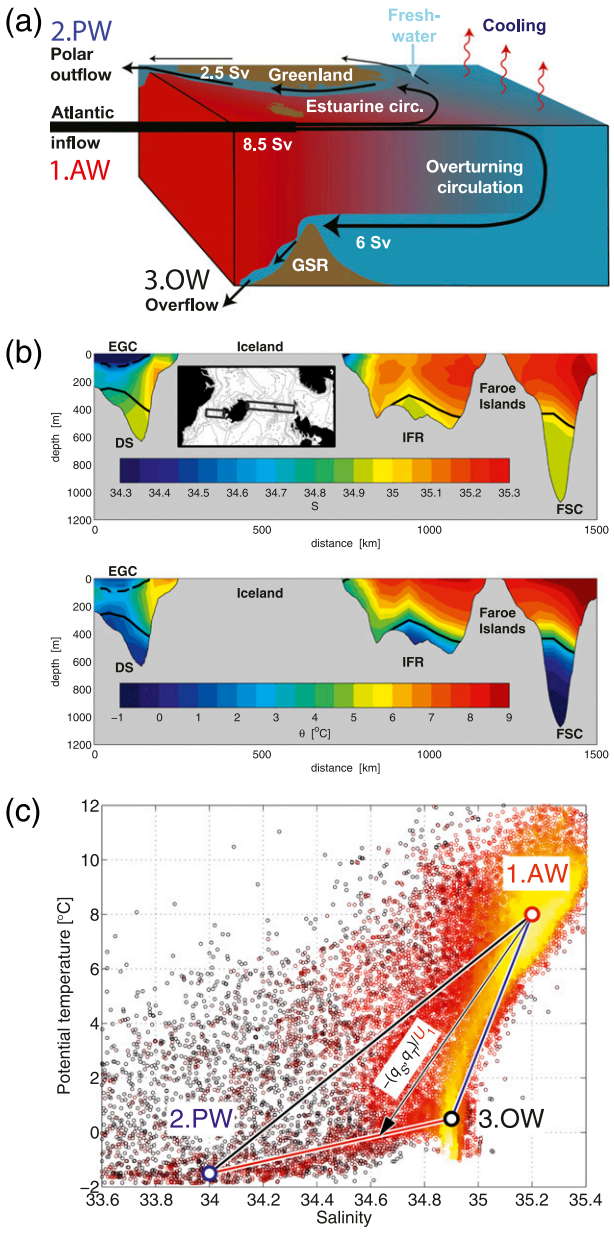

FIG. 1. The Arctic–Atlantic thermohaline circulation. (a) Schematic of the estuarine and overturning circulations constituting the Arctic–Atlantic THC [adaptation of original figure (Hansen et al. 2008) courtesy of B. Hansen]. (b) Climatology of GSR salinity and potential temperature (see inlet figure for the sampling domain). The extent of polar outflow with the East Greenland Current (EGC) is indicated by the 34.5 isohaline (stippled), and the extent of overflow is indicated by the 27.8 isopycnal (solid). (c) The reference AW–PW–OW thermohaline triangle and the projected forcing [Table 1; (7)]. The background *TS* scatter is the more than 300 000 hydrographic observations constituting the climatology (1950–2005; Nilsen et al. 2008). The color scale indicates the density of observations; for visibility, only 1/20th of the data points east of Iceland have been plotted.

north of GSR tend to be concerned with the overturning from inflow to dense overflow (Hansen and Østerhus 2000; Mauritzen 1996; Isachsen et al. 2007), neglecting the role of a variable polar outflow with the East Greenland Current.

Admittedly, several authors have described the circulation of the Arctic Mediterranean as a so-called double estuary (Stigebrandt 1985; Carmack 2007; Rudels 2010); the heat loss and consequent dense water formation in the Nordic Seas constitute an overturning circulation (or negative estuary), while farther north freshwater input maintains an estuarine circulation in line with Knudsen's (1900) original concept: that is, freshwater forcing accommodates Atlantic inflow (a positive estuary). It nevertheless appears that our study provides the first analytical framework that accounts for the coupled overturning and estuarine circulations of Atlantic inflow, polar outflow, and dense overflow (Fig. 1), thus allowing for the THC's generic two degrees of freedom.

2. A simple model

We utilize the observed three-layered structure of the Arctic–Atlantic THC to derive explicit expressions for the associated volume transports across GSR. The approach is simplified to the extent that dynamics (e.g., Straneo 2006; Spall 2012) is bypassed; the THC's observed layering into inflow, polar outflow, and overflow (Fig. 1) is assumed a priori. To construct a simple (or the simplest) model of three-layered THC, we add heat to the well-known Knudsen (1900) equations that have been used to estimate estuarine circulation from freshwater input for more than a century. By including a heat budget, both the estuarine circulation with transformation of AW into PW and the overturning of AW into OW—the negative estuary—can be considered simultaneously,

$$U_1 + U_2 + U_3 = 0, \tag{1}$$

$$S_1U_1 + S_2U_2 + S_3U_3 = q_S, \tag{2}$$

$$T_1U_1 + T_2U_2 + T_3U_3 = q_T, \tag{3}$$

where U_i is volume transport into the Arctic Mediterranean and S_i and T_i are salinity and potential temperature of the AW, PW, and OW layers ($i = 1$, 2, and 3). The virtual salt flux q_S and temperature flux q_T out of the ocean are the Arctic Mediterranean buoyancy forcing that balances the advective transports across GSR. Changing ocean storage of salt and heat adds to $q_{S,T}$ in the general transient case as discussed in the appendix, where we argue that a balance of ocean advection and

buoyancy forcing can be expected at decadal time scales and beyond. [There is also a relatively moderate contribution from eddy transport across GSR (Hansen and Østerhus 2000), but this is not explicitly considered here.] Note that the volume transports relate linearly to the buoyancy forcing, thus U_i and $q_{S,T}$ can equally well be considered anomalies in (1)–(3).

Explicit expressions for the volume transports follow from inverting (1)–(3),

$$U_1 = \frac{(T_2 - T_3)q_S - (S_2 - S_3)q_T}{\Delta}, \tag{4}$$

$$U_2 = \frac{(T_3 - T_1)q_S - (S_3 - S_1)q_T}{\Delta}, \tag{5}$$

$$U_3 = \frac{(T_1 - T_2)q_S - (S_1 - S_2)q_T}{\Delta}, \tag{6}$$

with $\Delta = (S_1 - S_2)(T_1 - T_3) - (S_1 - S_3)(T_1 - T_2)$. The functional dependence does not imply causality, it simply diagnoses—from first principles—the volume transports consistent with observed or estimated GSR hydrography and buoyancy forcing. The determinant Δ is twice the area of the AW–PW–OW "thermohaline triangle," a measure of the total water mass contrast at GSR (Fig. 1c).

3. The Arctic–Atlantic THC constrained

The conservation (1)–(3) is manifested in observed hydrography as follows: Buoyancy forcing transforms AW into a net outflow water mass residing on the PW–OW mixing line according to the outflow's division into polar outflow and dense overflow (Fig. 1c). The volume transport of a water mass thus equals the area spanned out by the forcing vector and the thermohaline contrast of the other two water masses, divided by Δ [cf. (4)–(6)]. There is consequently no change in inflow, polar outflow, and overflow for anomalous forcing aligned with PW–OW, AW–OW, and AW–PW mixing lines, respectively: that is, for $dq_T/dq_S = (T_i - T_j)/(S_i - S_j)$, $i \neq j$. The slope of mixing lines thus translates directly between S,T space and $q_{S,T}$ space (cf. Fig. 2). The term "mixing line"—in lack of a more precise standard term—refers to the contrast of water masses and not to actual mixing at GSR; it is the water mass transformation north of GSR that converts AW into PW and OW.

The model THC is maybe best illustrated by the volume transports as constrained by freshwater input and heat loss (Fig. 2, left column; assuming reference hydrography: Table 1). The reference transports are realized for

$$F^{\mathrm{ref}} = 0.14\,\mathrm{Sv}, \quad Q^{\mathrm{ref}} = 282\,\mathrm{TW}, \tag{7}$$

which are compatible with climatological estimates of the buoyancy forcing for the Arctic Mediterranean (Mauritzen 1996; Dickson et al. 2007; Simonsen and Haugan 1996). Modeled transports can therefore be considered realistic with respect to the observed mean Arctic–Atlantic THC (see also the appendix). The conversion between fluxes $q_{S,T}$ and freshwater input and heat loss is that it requires 0.029 Sv ($1\,\mathrm{Sv} \equiv 10^6\,\mathrm{m^3\,s^{-1}}$) of freshwater input to freshen a 1-Sv flow by 1 practical salinity unit and a 4.1-TW heat loss to cool 1 Sv by 1°C, respectively. Note that F^{ref} only accounts for the freshwater consumed by water mass transformation north of GSR: that is, freshwater input less net sea ice export.

Isolines of constant flow are aligned with GSR mixing lines as inferred from (4)–(6). The operation of the Arctic–Atlantic THC—AW in and PW and OW out—requires a buoyancy forcing restricted by the mixing lines AW–OW ($U_2 = 0$) and AW–PW ($U_3 = 0$). The exemplified responses to freshwater (FW) and to heat (COOL) are shown by vectors, with the former being an estimate (0.03 Sv) of anomalous pan-Arctic freshwater input since the 1960s (Peterson et al. 2006; Dyurgerov et al. 2010) and the latter simply scaled to 62 TW so that the combination of the two (REF) is aligned with the reference forcing [Eq. (7)]. Note that the scaling of axes in Fig. 2 reflects GSR hydrography in present climate (Fig. 1c). The qualitative alignment of isolines is nevertheless independent of the specific scaling; the PW–OW mixing line is generically the more isothermal and AW–OW is the more isohaline. The inflow is thus more dependent on heat loss, polar outflow is more dependent on freshwater input, and overflow reflects both from continuity.

4. Implied sensitivity

The left column of Fig. 2 is a generic representation of the THC's response to change in freshwater and heat budgets. The corresponding dependence on water mass properties follows from scaling the dependence on buoyancy forcing with the volume transport carrying the water mass in question. It results straightforwardly from partial derivation of (4)–(6) that

$$\frac{\partial U_i}{\partial S_j} = -U_j\frac{\partial U_i}{\partial q_S}, \quad \frac{\partial U_i}{\partial T_j} = -U_j\frac{\partial U_i}{\partial q_T}, \tag{8}$$

for the dependence of transports $i = 1, 2$, and 3 on water masses $j = 1, 2$, and 3. (Note that outflow is defined as negative transport.) Decreasing AW, increasing PW, or increasing OW salinity (temperature) is thus effectively the same as increasing the freshwater input (heat loss). This simply reflects that the inflow is the Arctic Mediterranean's

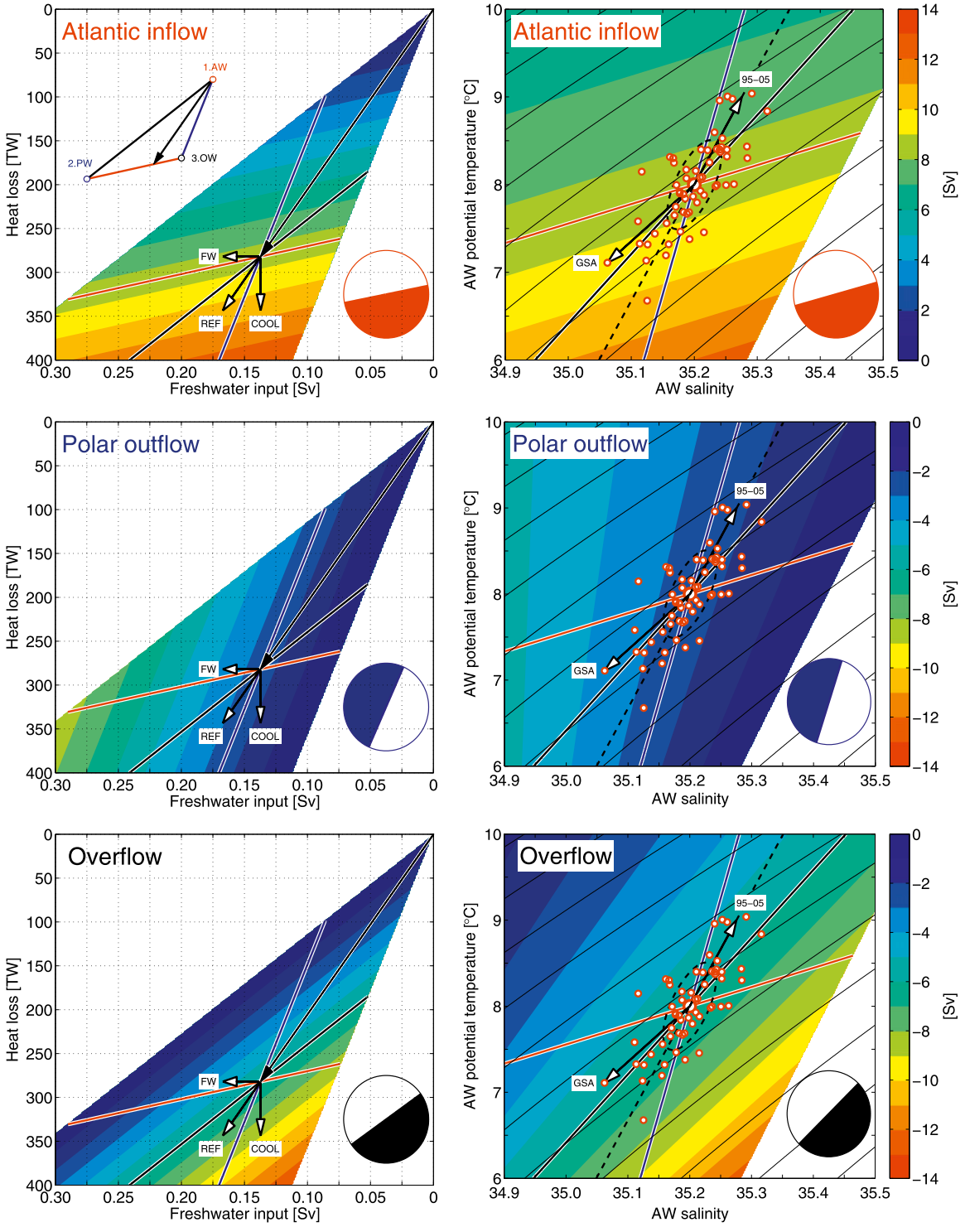

FIG. 2. Northern constraints on the thermohaline circulation. The color shading indicates volume transports (in Sv) as constrained by (left) freshwater input and heat loss and (right) inflow salinity and potential temperature. Northward transport is positive, and coordinate axes are scaled consistent with present climate (cf. inlet figure top left and Fig. 1c). The colored (white) semicircles are simple visualizations of the thermohaline alignment of positive (negative) transport anomalies; see also Fig. 3. The *TS* scatter in the right column (red circles) is observed annual AW hydrography for 1950–2005 (Eldevik et al. 2009), and the broken curves give the associated linear regression and variance ellipse; black contour lines are isopycnals with a spacing of 0.01 kg m^{-3}. Perturbations FW, COOL, REF, GSA, and 95–05 are discussed in the main text.

TABLE 1. Reference hydrography and THC sensitivity: observation-based reference salinities S_i^{ref}, potential temperatures T_i^{ref}, and volume transports U_i^{ref} at GSR (cf. Rudels et al. 1999; Hansen and Østerhus 2000; Hansen et al. 2008; Nilsson et al. 2008; Eldevik et al. 2009) and the partial derivatives of the volume transports (4)–(6) with respect to the thermohaline properties for the reference values. Inflow is defined as positive, and negative outflow derivatives thus mean increased outflow.

Water mass	i	S_i^{ref}	T_i^{ref} °C	U_i^{ref} Sv	$\partial U_i/\partial F$ Sv Sv^{-1}	$\partial U_i/\partial Q$ Sv TW^{-1}	$\partial U_i/\partial S_1$	$\partial U_i/\partial S_2$ Sv	$\partial U_i/\partial S_3$	$\partial U_i/\partial T_1$	$\partial U_i/\partial T_2$ Sv °C^{-1}	$\partial U_i/\partial T_3$
AW	1	35.2	8.0	8.5	−11	+0.036	+2.8	−0.8	−2.0	−1.24	+0.37	+0.88
PW	2	34.0	−1.5	−2.5	−43	+0.012	+10.4	−3.0	−7.3	−0.41	+0.12	+0.29
OW	3	34.9	0.5	−6.0	+54	−0.048	−13.1	+3.9	+9.3	+1.66	−0.49	−1.17

source of salt and heat, while the outflows and the buoyancy forcing are the sinks (cf. Fig. 2 and Table 1).

The above is exemplified by the right column of Fig. 2, displaying anomalous THC contributed by variable AW (assuming reference PW, OW, and buoyancy forcing). In the scatter of observed AW variability, the ''Great Salinity Anomaly'' (GSA; Dickson et al. 1988) of the 1970s and the recent decade of salinification and warming of 1995–2005 (95–05; Holliday et al. 2008) are shown by vectors. Note particularly how the thermohaline contrasts at GSR again constrain the character of THC change (compare the two columns of Fig. 2). The similar dependences on OW and PW are not shown, but the linear response to change in each thermohaline property is quantified in Table 1.

A reduced inflow is commonly related to a reduced overflow (Curry and Mauritzen 2005; Hansen et al. 2008). The qualitative relation is seen to hold when considering the freshwater and heat budgets separately (FW and COOL; Fig. 2, left), which is consistent with a density-driven overturning circulation (Kuhlbrodt et al. 2007). Observed AW variability, however, is largely density compensated (cf. Fig. 2, right). Figure 2 and Table 1 illustrate that both the polar outflow and the dense overflow must be accounted for to constrain the inflow. This is clearly exemplified by the hypothetical case of a persistent GSA-like shift in AW. This shift that is almost perfectly density compensated, will in particular contribute to *increased* inflow and *decreased* overflow.

5. Arctic–Atlantic tit for tat

The conclusion of the previous section points to an important and hopefully useful aspect of our suggested framework: it can be used for closed and quantitative inference on THC change relating to observed or hypothesized change in a given or several thermohaline properties.

A freshening of the overflow is, for example, often considered indicative of a weaker overflow (e.g., Dickson et al. 2002). The inference is not correct as is stands; it is conditioned on additional change in other thermohaline properties. A reduction of OW salinity by, for example, 0.1, with all else equal, is from the diagnosis (4)–(6) consistent with a 1.1-Sv strengthening of the overflow (0.2-Sv strengthening of inflow; 0.9-Sv weakening of polar outflow) with respect to the reference state. This is the advective adjustment required to maintain the basin's salt budget.

Increased freshwater input is one possible cause for fresher overflow (in addition to the advective adjustment inferred above). If one hypothesizes that the OW freshening results from increased freshwater input, one finds that a 0.017-Sv increase in freshwater input added to the exemplified OW freshening counterbalances the need for advective adjustment in (4)–(6): that is, there is no change in THC. A causal and anomalous freshwater input in excess of 0.017 Sv is thus required to infer a weaker overflow in this example (assuming an unperturbed heat budget and no change in AW and PW salinities).

Another timely example is the recent—and expected future—decline in Arctic sea ice cover, whose relation to THC appears unresolved (Serreze et al. 2007). The wintertime loss of Arctic sea ice is most pronounced in the Barents Sea, where a retreating ice cover reflects increased Atlantic inflow locally (Helland-Hansen and Nansen 1909; Smedsrud et al. 2013), and a heat loss increase of 138 W m^{-2} has been associated with the sea ice retreat (Årthun et al. 2012). For the annual mean area decrease since the late 1960s, about 4×10^5 km^2 (Kvingedal 2005), the loss corresponds to COOL (Fig. 2). Combined with the pan-Arctic freshwater input anomaly for the same period (FW), the heat loss accommodates a proportional strengthening of THC similar to REF (Fig. 2).

Note again that this section is about making closed and consistent inference on THC change associated with any specified change in thermohaline properties (effectively REF in the last case). All properties will in reality be variable to a greater or lesser extent. This synoptic covariability, including that of volume transports, is not known from observations. Any ''reconstructed'' THC change (4)–(6) can only account for the subset of variability that has been observed; what is unobserved must by necessity be assumed constant or otherwise reasonably

hypothesized. The linear sensitivity of Arctic–Atlantic THC to all model variables in present climate is quantified in Table 1 for completeness and an easy reference to the magnitudes involved. Consulting this lookup table would slightly underestimate the change associated with fresher overflow exemplified above, as the table does not account for nonlinearity. Note that the table's $\partial U_i/\partial F$ and $\partial U_i/\partial Q$ columns (visualized in Fig. 2, left column) are not approximate sensitivities since model volume transports relate linearly to buoyancy forcing.

6. Concluding remarks

The thermohaline contrasts of the exchanges across GSR (Fig. 1c) are at the heart of our Arctic–Atlantic THC model. The contrasts divide the buoyancy forcing plane (or *TS* plane) into six distinct regimes of anomalous Atlantic inflow, polar outflow, and dense overflow (Fig. 2). Figure 3 summarizes this qualitative sensitivity that only depends on the alignment of thermohaline anomalies and not their magnitude. Change in THC strength (the inflow) primarily resides with the heat budget. To what extent a change is more estuarine (polar outflow), overturning (overflow), or both depends on the simultaneous change in the freshwater budget. The sensitivity can be inferred directly from Fig. 1c; the strength of a warm inflow that is balanced by two outflows of similar cold temperature is essentially determined from heat loss alone. An alternative general summary of Fig. 3 is the following: The heat sensitivity of THC is poorly constrained within the framework of an estuarine circulation as the approach neglects the simultaneous contribution from overturning, which is more—and oppositely—sensitive to heat. It is equally inappropriate to assess freshwater sensitivity by approximating Arctic–Atlantic THC as an overturning circulation alone.

We have suggested a simple but consistent framework to assess the Arctic–Atlantic THC both qualitatively (Fig. 3) and quantitatively (Fig. 2 and Table 1). Concerning the quantitative aspect, the less the total water mass contrast at GSR (quantified by Δ), the more sensitive the THC is to changing buoyancy forcing or hydrography [cf. (4)–(6) and (8); volume transports are inversely proportional to Δ]. The above implies that climates—or climate model projections—that differ distinctly in water masses at GSR can be expected to differ distinctly in their THC characteristics and thus the climate variability and sensitivity associated. The instrumental record shows warmer and more saline inflow (Holliday et al. 2008), comparatively constant overflow hydrography (Eldevik et al. 2009), and likely fresher polar outflow (Curry and Mauritzen 2005) since the 1970s. This trend of increasing thermohaline contrasts at GSR suggests a more robust Arctic–Atlantic THC from recent climate change.

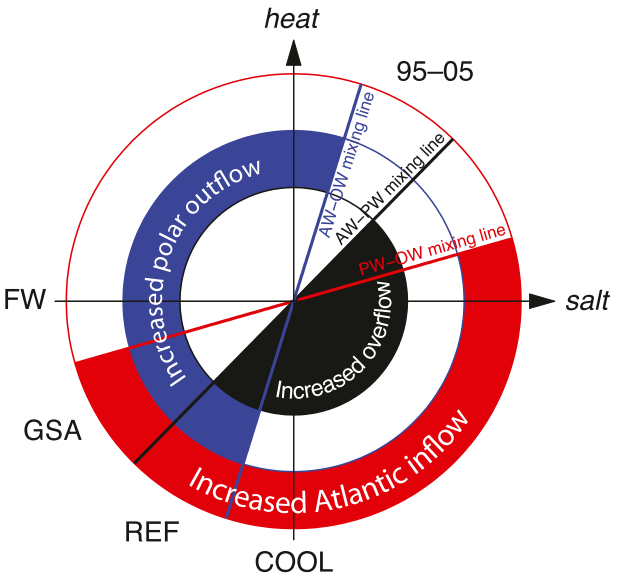

FIG. 3. The qualitative sensitivity of the Arctic–Atlantic thermohaline circulation. The thermohaline contrasts of the circulation divide THC change into six distinct regimes defined by the haline (horizontal axis) vs thermal (vertical) change in buoyancy forcing or GSR water masses. This "wheel of change" results from superimposing the colored semicircles defining positive and negative anomalies in Fig. 2, and the labeled regimes correspond to the perturbations exemplified in this figure.

Acknowledgments. This research was supported by the Research Council of Norway through the projects BIAC, NorClim, and POCAHONTAS and by EU FP7 through the project THOR. The observational data were provided by the Marine Research Institute, Iceland; Institute of Marine Research, Norway; the Faroese Fisheries Laboratory; and the Geophysical Institute, University of Bergen, Norway, through the NISE project. The authors are grateful for discussions with numerous colleagues and the constructive suggestions of the reviewers.

APPENDIX

On Model Validity

Apart from the three-layered structure (which is the common characterization and reasonable from observations: e.g., Fig. 1; Hansen and Østerhus 2000) and an Arctic Mediterranean with GSR as the only gateway [any Bering Strait influence (e.g., Woodgate et al. 2006) must be modeled as buoyancy forcing], the main model assumption is a dominant balance between external buoyancy forcing and the advection of heat and salt

through the gateway. This is appropriate for a mean climate or the quasi-stationary evolution of climate on centennial to geological time scales, but below a certain time-scale trends in storage generally cannot be neglected. [Note that this can be circumvented formally in our model by considering $q_{S,T}$ as the net contribution of buoyancy forcing and changing storage (e.g., in Fig. 1c), but this is practical only to the extent that this net can be estimated.]

A recent warming trend of 3 TW can be estimated from the observational record (1995–2010) for the Norwegian Sea, the main heat reservoir of the Arctic Mediterranean (Skagseth and Mork 2012). The decadal-scale trend associated with the observed freshening of the Nordic Seas since 1955 is about 0.003 Sv (Curry and Mauritzen 2005). A similar trend is also associated with the accumulation of freshwater in the Beaufort Gyre that has received much attention recently (Proshutinsky et al. 2009). These estimated trends in storage are two orders of magnitude less than the mean balance quantified by (7). This suggests that changing storage can be neglected for assessments on decadal time scales and beyond, at least in present climate. We note that ocean GCM simulations of an idealized Arctic Mediterranean, starting from rest, achieve balance between buoyancy forcing and ocean advection within 30 yr (Spall 2012).

REFERENCES

Årthun, M., T. Eldevik, L. H. Smedsrud, Ø. Skagseth, and R. Ingvaldsen, 2012: Quantifying the influence of Atlantic heat on Barents Sea ice variability and retreat. *J. Climate,* **25,** 4736–4743.

Carmack, E. C., 2007: The alpha/beta ocean distinction: A perspective on freshwater fluxes, convection, nutrients and productivity in high-latitude seas. *Deep-Sea Res. II,* **54,** 2578–2598.

Curry, R., and C. Mauritzen, 2005: Dilution of the northern North Atlantic Ocean in recent decades. *Science,* **308,** 1772–1774.

Dickson, B., I. Yashayaev, J. Meincke, B. Turrell, S. Dye, and J. Holfort, 2002: Rapid freshening of the deep North Atlantic Ocean over the past four decades. *Nature,* **416,** 832–837.

Dickson, R. R., J. Meincke, S.-A. Malmberg, and A. J. Lee, 1988: The Great Salinity Anomaly in the northern North Atlantic 1968–1982. *Prog. Oceanogr.,* **20,** 103–151.

——, B. Rudels, S. Dye, M. Karcher, J. Meincke, and I. Yashayaev, 2007: Current estimates of freshwater flux through Arctic and subarctic seas. *Prog. Oceanogr.,* **73,** 210–230.

Dyurgerov, M., A. Bring, and G. Destouni, 2010: Integrated assessment of changes in freshwater inflow to the Arctic Ocean. *J. Geophys. Res.,* **115,** D12116, doi:10.1029/2009JD013060.

Eldevik, T., J. E. Ø. Nilsen, D. Iovino, K. A. Olsson, A. B. Sandø, and H. Drange, 2009: Observed sources and variability of Nordic Seas overflow. *Nat. Geosci.,* **2,** 406–410.

Hansen, B., and S. Østerhus, 2000: North Atlantic–Nordic Seas exchanges. *Prog. Oceanogr.,* **45,** 109–208.

——, ——, W. R. Turrell, S. Jónsson, H. Valdimarsson, H. Hátún, and S. M. Olsen, 2008: The inflow of Atlantic water, heat and salt across the Greenland-Scotland ridge. *Arctic–Subarctic Ocean Fluxes: Defining the Role of the Northern Seas in Climate,* B. Dickson, J. Meincke, and P. Rhines, Eds., Springer Verlag, 15–44.

Helland-Hansen, B., and F. Nansen, 1909: The Norwegian Sea: Its physical oceanography based upon the Norwegian researches 1900–1904. Norwegian Fishery and Marine Investigations Rep. Vol. 2, Part 1, No. 2, 390 pp.

Holliday, N. P., and Coauthors, 2008: Reversal of the 1960s to 1990s freshening trend in the northeast North Atlantic and Nordic Seas. *Geophys. Res. Lett.,* **35,** L03614, doi:10.1029/2007GL032675.

Isachsen, P. E., C. Mauritzen, and H. Svendsen, 2007: Dense water formation in the Nordic Seas diagnosed from sea surface buoyancy flux. *Deep-Sea Res.,* **54,** 22–41.

Knudsen, M., 1900: Ein hydrographisher Lehrsats. *Ann. Hydr. Mar. Meteor.,* **28,** 316–320.

Kuhlbrodt, T., A. Griesel, M. Montoya, A. Levermann, M. Hofmann, and S. Rahmstorf, 2007: On the driving processes of the Atlantic meridional overturning circulation. *Rev. Geophys.,* **45,** RG2001, doi:10.1029/2004RG000166.

Kvingedal, B., 2005: Sea-ice extent and variability in the Nordic Seas, 1967-2002. *The Nordic Seas: An Integrated Perspective, Geophys. Monogr.,* Vol. 158, Amer. Geophys. Union, 39–49.

Lynch-Stieglitz, J., and Coauthors, 2007: Atlantic meridional overturning circulation during the Last Glacial Maximum. *Science,* **316,** 66–69.

Mauritzen, C., 1996: Production of dense overflow waters feeding the North Atlantic across the Greenland-Scotland ridge. Part 2: An inverse model. *Deep-Sea Res. I,* **43,** 807–835.

Nilsen, J. E. Ø., H. Hátún, K. A. Mork, and H. Valdimarsson, 2008: The NISE data set. Faroese Fisheries Laboratory Tech. Rep. 08-01, 20 pp.

Nilsson, J., G. Björk, B. Rudels, P. Winsor, and D. Torres, 2008: Liquid freshwater transport and polar surface water characteristics in the East Greenland Current during the AO-02 Oden expedition. *Prog. Oceanogr.,* **78,** 45–57.

Peterson, B. J., J. McClelland, R. Curry, R. M. Holmes, J. E. Walsh, and K. Aagaard, 2006: Trajectory shifts in the Arctic and Subarctic freshwater cycle. *Science,* **313,** 1061–1066.

Proshutinsky, A., and Coauthors, 2009: Beaufort gyre freshwater reservoir: State and variability from observations. *J. Geophys. Res.,* **114,** C00A10, doi:10.1029/2008JC005104.

Quadfasel, D., and R. Käse, 2007: Present-day manifestation of the Nordic Seas overflows. *Ocean Circulation: Mechanisms and Impacts, Geophys. Monogr.,* Vol. 173, Amer. Geophys. Union, 75–90.

Rahmstorf, S., 1996: On the freshwater forcing and transport of the Atlantic thermohaline circulation. *Climate Dyn.,* **12,** 799–811.

Rhines, P., S. Häkkinen, and S. A. Josey, 2008: Is oceanic heat transport significant in the climate system? *Arctic–Subarctic Ocean Fluxes: Defining the Role of the Northern Seas in Climate,* B. Dickson, J. Meincke, and P. Rhines, Eds., Springer Verlag, 87–109.

Rudels, B., 2010: Constraints on exchanges in the Arctic Mediterranean—Do they exist and can they be of use? *Tellus,* **62A,** 109–122.

——, H. J. Friedrich, and D. Quadfasel, 1999: The Arctic circumpolar boundary current. *Deep-Sea Res. II,* **46,** 1023–1062.

Serreze, M. C., M. M. Holland, and J. Stroeve, 2007: Perspectives on the Arctic's shrinking sea-ice cover. *Science,* **315,** 1533–1536.

Simonsen, K., and P. H. Haugan, 1996: Heat budgets of the Arctic Mediterranean and sea surface heat flux parameterizations for the Nordic Seas. *J. Geophys. Res.,* **101** (C3), 6553–6576.

Skagseth, Ø., and K. A. Mork, 2012: Heat content in the Norwegian Sea, 1995–2010. *ICES J. Mar. Sci.,* **69,** 826–832.

Smedsrud, L. H., and Coauthors, 2013: The role of the Barents Sea in the Arctic climate system. *Rev. Geophys.,* doi:10.1002/rog.20017, in press.

Spall, M. A., 2012: Influences of precipitation on water mass transformation and deep convection. *J. Phys. Oceanogr.,* **42,** 1684–1700.

Spielhagen, R. F., and Coauthors, 2011: Enhanced modern heat transfer to the Arctic by warm Atlantic water. *Science,* **331,** 450–453.

Stigebrandt, A., 1985: On the hydrographic and ice conditions in the northern North Atlantic during different phases of a glaciation cycle. *Palaeogeogr. Palaeoclimatol. Palaeoecol.,* **50,** 303–321.

Straneo, F., 2006: Heat and freshwater transport through the central Labrador Sea. *J. Phys. Oceanogr.,* **36,** 606–628.

Woodgate, R. A., K. Aagaard, and T. J. Weingartner, 2006: Interannual changes in the Bering Strait fluxes of volume, heat and freshwater between 1991 and 2004. *Geophys. Res. Lett.,* **33,** L15609, doi:10.1029/2006GL026931.

Wunsch, C., 2002: What is the thermohaline circulation? *Science,* **298,** 1179–1181.